Inverse-based ultrasound imaging through linear programming

***Abstract*—Ultrasound image reconstruction is typically performed through delay-and-sum: they are linear and computationally efficient algorithms. However, images produced by this family of methods contain oscillation that limits the imaging resolution–a phenomenon especially problematic when imaging very close point-like reflectors. Inverse-based methods have been proven to enhance imaging resolution by reducing high-frequency oscillations. They incorporate specific prior information and reduce oscillations by proper regularization. Although the regularization reduces oscillations, it also attenuates the signal of interest. We are proposing an inverse-based method without regularization. It is a linear programming-based approach: the inverse-problem is modeled as the minimization of the ℓ_1 norm of a residue, which is solved through linear programming. We compared our methods to delay-and-sum and inverse-based imaging algorithms by simulating a steel specimen with point-like reflectors. Our method outperforms classical algorithms regarding SNR and resolution but at a higher computational cost.**

***Index Terms*—Acoustic signal processing, inverse-problem, non-destructive testing (NDT), ultrasonic imaging**

I. Introduction

Ultrasonic imaging is a safe and cost-effective method widely applied in non-destructive testing (NDT). The most common probe technology are phased arrays–an arrangement comprised of dozens of elements capable of acting as an emitter or receiver of ultrasound signal.

Delay and sum (DAS) algorithms are the common choice for ultrasonic imaging; they apply a specific time delay to each received signal to sum them coherently. The total focusing method (TFM) is the gold standard when it comes to DAS. Although TFM is a fast and memory-efficient algorithm, its resolution is limited by Rayleigh criterion [1] and requires a higher number of channels to work properly [2].

Another imaging paradigm is inverse-based methods. They model the ultrasound propagation as a forward problem (e.g., a linear system), then reconstruct the image by solving the inverse problem (e.g., through least squares) [2]–[4]. Compared to DAS, they enhance imaging resolution [4] and decrease the data size requirements [2].

Although inverse-based methods solve some DAS pitfalls, they usually rely on regularization techniques to aggregate prior information into the imaging problem. Regularization techniques generally improve the imaging quality, but at the cost of reducing the desired signal energy [5], which worsens the signal-to-noise ratio.

We are proposing a new inverse-based method that does not require any regularization. Our method models the inverse-problem into a linear system of equations and solves it by minimizing an ℓ_1 norm of the residue. Then, we linearized the ℓ_1 norm and cast the problem as a linear programming problem.

II. Ultrasound Inspection

Ultrasound waves propagate in solids through different modes, but we are only interested in the pressure field in this paper. Waves that propagate by changing the pressure field are called longitudinal waves. Ultrasound transducers can generate spherical waves from an input electrical signal and vice-versa.

The most complete way of capturing ultrasound data from a phased-array transducer is called *Full Matrix Capture* (FMC). In this acquisition scheme, an element acts as a spherical wave source (or emitter), while the others act as receivers. This procedure is repeated until every element has acted as an emitter. The result is a data structure with size $N_t \times N_{\text{emitters}} \times N_{\text{receivers}}$ that belongs to $\mathbb{R}^1$, where N_t is the number of samples on the time-domain signal perceived by a single receiver. Since it is very common for an element to be able to act as a receiver or emitter (at different moments in time), $N_{\text{receivers}} = N_{\text{emitters}} = N_{\text{el}}$.

Our model deals with a vector version of the FMC: all columns are stacked to obtain a $N_t N_{\text{el}}^2 \times 1$ column-vector.

The transduction is considered ideal, hence the FMC data is numerically equal to the perceived acoustic pressure by transducer element.

III. Ultrasound Imaging

Suppose there is a linear phased array ultrasound transducer where each element can function as an emitter or receiver of ultrasound data. Working as an emitter, the element can emit a perfectly spherical wave originating at its center, or, as a receiver, it can receive a signal from any direction with the same amplitude. This transducer is in contact with an infinite-size specimen with longitudinal velocity c_l. In this medium, there is an ideal flaw: a point reflector with infinitesimal diameter and infinite depth (Fig 1).

Ultrasound imaging in NDT aims to reconstruct a 2-D image from data acquired by an ultrasound transducer. This allows us to estimate the presence and position of a possible flaw in the specimen.

IV. Modeling the Inverse Problem

Let $s_i(t)$ and $s_j(t)$ two $\mathbb{R}^1$ signals that represents acoustic pressure at i-th emitter ($\mathbf{x}_i$) and j-th receiver ($\mathbf{x}_j$). Assumed the time-invariance of $s(.)$, if there is a punctual reflector at $\mathbf{f}$ (Fig. 1) we can say that $s_j(t) = s_i(t - \tau)$, where τ is the time-of-flight between the emitter and receiver, i.e.,

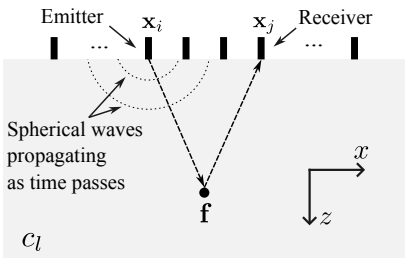

Fig. 1: A single firing event of a full-matrix capture, where the i-th element at $\mathbf{x}_i$ acts as emitter, and the j-th element at $\mathbf{x}_j$ as receiver. An ideal punctual reflector at $\mathbf{f}$ reflects energy in all directions, including towards the j-th receiver.

$$\tau = \frac{||\mathbf{x}_i - \mathbf{f}||^2 + ||\mathbf{f} - \mathbf{x}_j||^2}{c_l}. \tag{1}$$

A common representation used in ultrasonic imaging is the reflectivity map. A matrix $\mathbf{R}$ with size $N_{rows} \times N_{cols}$ that belongs to $\mathbb{R}^1$, have its entries (pixel) intensity proportional to the amount of energy reflected at that location in space towards the transducer. We considered a reflectivity field with normalized amplitude, i.e. $r_m \in [0, 1]$ for all $m = 1, 2, \ldots, N_{\text{rows}}N_{\text{cols}}$. In this notation, 0 represents the total absence of a reflector at a given location, while 1 indicates the presence of an ideal punctual reflector.

When multiple reflectors are present, both time-invariance and linearity hold, leading to the principle of superposition. This means that the ultrasonic response of the system with multiple reflectors can be represented as the direct sum of the individual responses from each reflector considered separately.

A. Proposed Method

Our method uses the superposition principle and its divided into three main steps:

1) Simulation of reference signals.
2) Real-world inspection.
3) Solving the inverse problem.

The first step is performing $N_{\text{rows}}N_{\text{cols}}$ simulations. They will serve as a foundation to construct the waveform matrix $\mathbf{H}$. In each simulation, there will be only one punctual reflector, differing only by its different position; each position is distributed in a grid pattern (Fig. 2a). The region occupied by the grid is called the region of interest (ROI) and will be the imaging region. For each simulation the result will be a flattened FMC $\mathbf{h}_m$ where $m = 1, 2, \ldots, N_{\text{rows}}N_{\text{cols}}$.

The second step is performing a real-world inspection. If there is a point-like reflector, the goal is to discover its position (Fig. 2b). The acquired ultrasound data is also a flattened FMC $\mathbf{g}$, hence it has similar dimensions to $\mathbf{h}_m$. If the point-like reflector is within the ROI and all the $N_{\text{rows}}N_{\text{cols}}$ simulations are representative enough, the superposition theorem implies

$$\mathbf{g} = \sum_{j=1}^{N_{\text{rows}}N_{\text{cols}}} \mathbf{h}_j \cdot r_j \tag{2}$$

or in a matrix notation

$$\mathbf{g} = \mathbf{H}\mathbf{r} \tag{3}$$

where $H = \begin{bmatrix}\mathbf{h}_1 & \mathbf{h}_2 & \ldots & \mathbf{h}_M\end{bmatrix}$ its called the waveform matrix and $\mathbf{r} = \begin{bmatrix}r_1 & r_2 & \ldots & r_M\end{bmatrix}^T$ its the reflectivity map $\mathbf{R}$ that we wish to estimate (Fig. (2c)).

The third step is solving 3 is by minimizing the residue ℓ_1 norm:

$$\min_{\mathbf{r}} ||\mathbf{g} - \mathbf{H}\mathbf{r}||_1 = ||\mathbf{e}||_1 \tag{4}$$

where

$$\mathbf{e} = \begin{bmatrix} e_1 \\ \vdots \\ e_N \end{bmatrix} = \begin{bmatrix} g_1 - \sum_{j=1}^{N_{\text{rows}}N_{\text{cols}}}(H_{1j}r_j) \\ \vdots \\ g_N - \sum_{j=1}^{N_{\text{rows}}N_{\text{cols}}}(H_{Nj}r_j) \end{bmatrix} \tag{5}$$

Inverse-based imaging methods commonly employ ℓ_2 cost-function, as many numerical methods exist to efficiently solve the problem. We used an ℓ_1 cost-function that, although it requires special numerical methods to be solved, is known to promote solution sparsity [6]–a desired feature especially when imaging point-like reflectors.

The ℓ_1 is a piecewise linear function, thus if we split e_i into a positive e_{i+} and e_{i-} parts:

$$\mathbf{e}_{i+} = \begin{cases} e_i & \text{if } e_i > 0 \\ 0 & \text{otherwise} \end{cases} \tag{6}$$

and

$$\mathbf{e}_{i-} = \begin{cases} -e_i & \text{if } e_i < 0 \\ 0 & \text{otherwise} \end{cases} \tag{7}$$

will be linear functions.

The problem as stated at (5) along with Eq. (6) and (6) could be tackled by linear programming techniques.

B. Linear Programming

The splitting showed in Eq. (6) e (7) is achievable through two constrains:

$$e_{i+} \geq e_i \tag{8a}$$
$$e_{i-} \geq -e_i \tag{8b}$$

where $e_{i-} > 0$ e $e_{i+} > 0$. Finally, the problem is stated as:

$$\min_{x_j, e_{i+}, e_{i-}} \quad \sum_{i=1}^{N_{\text{t}}N_{\text{el}}^2} (e_{i+} + e_{i-})$$

$$\text{s.t.} \quad e_{i+} \geq \left[b_i - \sum_{j=1}^{M} (A_{ij}x_j) \right], \tag{9a}$$

$$e_{i-} \geq -\left[b_i - \sum_{j=1}^{M} (A_{ij}x_j) \right], \tag{9b}$$

$$1 \geq \quad x_j \quad \geq 0 \tag{9c}$$

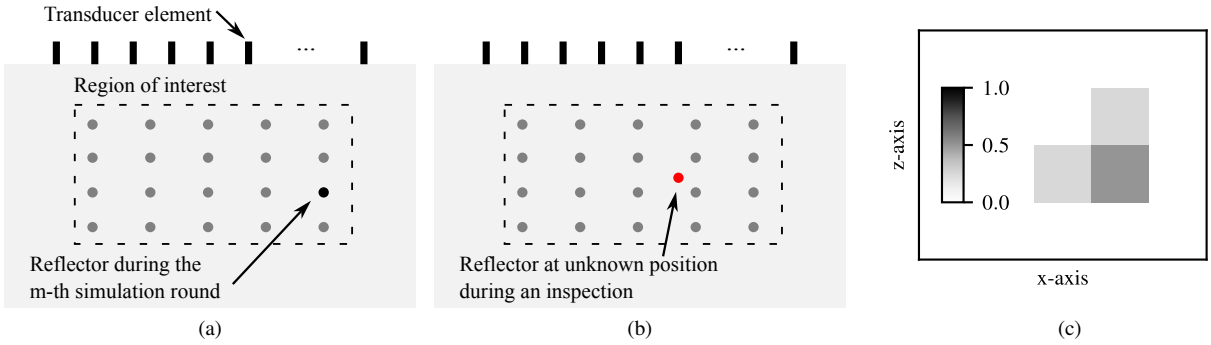

Fig. 2: Proposed method steps. (a) Simulation phase; (b) Real-world inspection phase; (c) Expected reflectivity field (linear scale).

for all $i = 1, 2, \ldots, N_{\mathrm{t}} N_{\mathrm{el}}^2$ and $j = 1, 2, \ldots, M$

V. Experiment and Results

In this section, we propose an experiment to test our method against two state-of-the-art ultrasound imaging methods. The first is an inverse-based method proposed by Laroche et al. [4], where Eq. (3) is solved through regularized least squares. The second is the TFM [7], a delay-and-sum algorithm widely used in ultrasound imaging, applied to non-destructive testing.

The experiment was a simulation meant to mimic a real-world inspection. The transducer is ideally coupled to an infinite steel specimen ($c = 5900\,\mathrm{m/s}$) with punctual reflectors; thus, the latter is the only source of reflection. The transducer is a linear phased array with 32 elements, a central frequency of $f_c = 1\,\mathrm{MHz}$, and an inter-element distance (pitch) of $p = 1.0\,\mathrm{mm}$. The transducer acoustic response $s(.)$ is a Gaussian wave with $40\,\%$ bandwidth ratio at $-6\,\mathrm{dB}$.

We simulated the interval of $0\,\mu\mathrm{s}$ to $10\,\mu\mathrm{s}$ at a sampling frequency of $f_s = 5 f_c$. To simulate background noise, we added a Gaussian noise to the acoustic spatial response with zero mean and 150×10^{-3} standard deviation. Since the acoustic pressure is normalized and the transduction phenomenon is ideal, the unit of the simulated ultrasound signal (and noise) could be interpreted as acoustic pressure or voltage.

The imaging ROI is a rectangle along the zx plane with $6\,\mathrm{mm}$ width and $7\,\mathrm{mm}$ height, with its center at $(3, 3.5)\mathrm{mm}$. The pixel size is $(0.5 \times 0.5)\mathrm{mm}$, resulting in a image of size (12×14) pixels.

Two punctual reflectors were placed at $\mathbf{f}_1 = (1.67, 3.67)\mathrm{mm}$ and $\mathbf{f}_2 = (-2, 5)\mathrm{mm}$. They do not perfectly align with any pixel from the simulated reflectivity map; hence, the experiment aims to evaluate the model's interpolation capability. The estimated reflectivity maps are shown in Fig 3.

VI. Discussion

Inverse-based methods (Fig 3a and 3b) resulted in far better qualitative results. Since ideal punctual reflectors (denoted by red circles) should yield infinitesimal reflectivity, the spread shown in the total focusing method reflectivity field translates to worse reconstruction quality and resolution, also confirmed by [2], [4]. Besides that, when compared side-by-side with the inverse-based methods, it is clear that regularization decreased the signal energy in Fig 3b; since this is not desired, it would lead to a worse signal-to-noise ratio. This would be critical in a noisy environment.

Although the results obtained by the proposed method were better, computational time was still a challenge. The proposed method runtime was $220\,\mathrm{s}$, while Laroche et al. was $1.68\,\mathrm{s}$ and total focusing method $0.35\,\mathrm{s}$. Linear programming solvers still require high runtime especially due to the fact that they are not easily implemented in parallel computing [8], while the two others have extensive CPU and GPU parallel implementation available.

VII. Conclusions

We proposed a new method for ultrasound imaging based on inverse problems. The inverse problem is a linear system of equations that we solve by minimizing the ℓ_1 of the residue. We took advantage of the fact that ℓ_1 is a piece-wise linear function and minimized through linear programming techniques. The experimental result shows good potential to enhance SNR when compared to traditional inverse-based methods and resolution when compared to delay and sum methods.

A. Future developments

The "real-world" ultrasound data used in this paper was simulated, therefore we strongly believe that it is vital to test the proposed method with real experimental results to evaluate its real performance. Furthermore, approaches to make the linear programming problem memory and time efficient are essential to decrease the pixel size and reproduce fully the results presented in the bibliography. A possible way to decrease the proposed method runtime is by firstly solving the ℓ_1 minimization through more efficient algorithms (e.g., iterative reweighted least squares [9]), then improving the obtained result through the proposed linear programming approach.

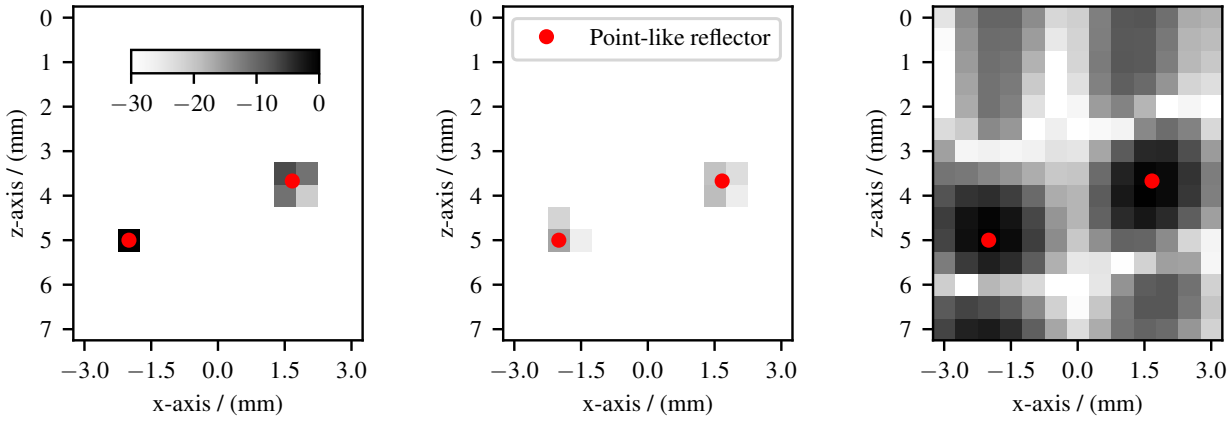

(a) (b) (c)

Fig. 3: Reflectivity field (logarithmic scale) comparison. (a) Proposed; (b) Laroche et al. [4]; (c) Total focusing method [7].

REFERENCES

[1] C. Fan, M. Caleap, M. Pan, B. W. Drinkwater, A comparison between ultrasonic array beamforming and super resolution imaging algorithms for non-destructive evaluation, Ultrasonics 54 (7) (2014) 1842–1850.

[2] F. T. Watt, A. Hauptmann, E. C. Mackle, E. Z. Zhang, P. C. Beard, E. J. Alles, Non-iterative model-based inversion for low channel-count optical ultrasound imaging, The Journal of the Acoustical Society of America 156 (5) (2024) 3514–3522.

[3] S. Wang, Y. Liu, J. Zhang, N. Jiang, M. Zhang, Inverse problem of ultrasound plane wave imaging with a low-rank and sparse model, in: 2024 IEEE Ultrasonics, Ferroelectrics, and Frequency Control Joint Symposium (UFFC-JS), IEEE, 2024, pp. 1–5.

[4] N. Laroche, S. Bourguignon, E. Carcreff, J. Idier, A. Duclos, An inverse approach for ultrasonic imaging from full matrix capture data: Application to resolution enhancement in ndt, IEEE transactions on ultrasonics, ferroelectrics, and frequency control 67 (9) (2020) 1877–1887.

[5] J. Idier, Bayesian approach to inverse problems, John Wiley & Sons, 2013.

[6] E. Ozkan, V. Vishnevsky, O. Goksel, Inverse problem of ultrasound beamforming with sparsity constraints and regularization, IEEE transactions on ultrasonics, ferroelectrics, and frequency control 65 (3) (2017) 356–365.

[7] C. Holmes, B. Drinkwater, P. Wilcox, The post-processing of ultrasonic array data using the total focusing method, Insight-Non-Destructive Testing and Condition Monitoring 46 (11) (2004) 677–680.

[8] M. Mirhosseini, M. Fazlali, M. K. Fallah, J.-A. Lee, A fast milp solver for high-level synthesis based on heuristic model reduction and enhanced branch and bound algorithm, The Journal of Supercomputing 79 (11) (2023) 12042–12073.

[9] P. W. Holland, R. E. Welsch, Robust regression using iteratively reweighted least-squares, Communications in Statistics-theory and Methods 6 (9) (1977) 813–827.